

*В автономних системах, що потребують компактного джерела електроенергії, а також при необхідності спрощення механізмів конструкції енергосистем, все більш широке застосування знаходять лінійні електрогенератори. Для дослідження характеристик лінійного електрогенератора запропонована аналітична модель його магнітоактивної частини. В основу моделі покладено припущення про періодичність лінійного поступального руху якоря відносно нерухомої циліндричної обмотки. На основі уявлення магнітного поля, яке створює якорь електрогенератора, циліндричними гармоніками скалярного потенціалу, проведено аналіз магнітного потоку, створюваного індуктором, конструкція якого містить кілька попарно-протилежно орієнтованих циліндричних постійних магнітів. Використання уявлень на основі циліндричних гармонік для магнітного потоку і ЕРС, яка наводиться в круговому контурі, дозволило обґрунтувати раціональну кількість циліндричних магнітів якоря і їх геометричні параметри. Проведено оцінку втрат, викликаних технологічною необхідністю застосування замість суцільних циліндричних магнітів кільцеподібних, з тими ж габаритними розмірами. Проведено аналіз втрат магнітного потокозчеплення зі струмовою обмоткою, що вишикають у зв'язку з наявністю технологічно необхідного зазору між постійними магнітами і секціями обмотки. Проведено аналіз розташування і комутації секцій обмоток, що дозволило обґрунтувати вибір раціонального розміру в поперечному перерізу. Для експериментальної перевірки аналітично отриманих результатів була створена фізична модель лінійного електрогенератора з якорем, що містить постійні циліндричні магніти, поступальний періодичне рух якого забезпечувався зовнішнім електроприводом. Аналіз зафіксованих за допомогою цифрового осцилографа залежностей ЕРС з невеликою (5 %) похибкою підтвердив отримані аналітичні результати і коректність покладених в основу моделі положень*

*Ключові слова: лінійний електрогенератор, магнітний потік, постійний магніт, електрорушійна сила, циліндрична гармоніка*

Received date 05.04.2020

Accepted date 08.06.2020

Published date 30.06.2020

## 1. Introduction

One of the current trends in the development of science and technology is expanding the scope of the practical application of linear electric generators of various types and purposes. For example, "green" power engineering in which a linear electric generator is used to convert the energy of sea waves is one of the areas of application [1]. Coupled with an internal combustion engine, a linear electric generator forms an energy system of various autonomous objects [2]. The advantages of this arrangement in the power plant configuration [3] include compact design, simplification of the mechanical part of the system, and its higher reliability due to exclusion of crank elements, etc. The choice of design options of the linear electric generator itself is possible. Its operation is based on inducing electromotive force (EMF) in windings during their displacement relative to the inductor [4]. In one embodiment, a fixed stator is used with a

# ANALYTICAL AND PHYSICAL MODELING OF THE MAGNETICALLY ACTIVE PART OF A LINEAR ELECTRIC GENERATOR WITH PERMANENT MAGNETS

UDC 621.313

DOI: 10.15587/1729-4061.2020.205154

**O. Rezinin**

Doctor of Technical Sciences, Professor  
Department of Engineering Electrophysics\*  
E-mail: orezynkin@gmail.com

**A. Getman**

Doctor of Technical Sciences, Senior Researcher  
Department of Theoretical Electrical Engineering\*  
E-mail: getmanav70@gmail.com

**S. Buryakovskiy**

Doctor of Technical Sciences, Professor  
Research and Design Institute "Molniya"\*  
E-mail: sergbyr@i.ua

**B. Kubrik**

PhD, Associate Professor  
Department of Theoretical Electrical Engineering\*  
E-mail: kubrikboris@gmail.com

\*National Technical University  
"Kharkiv Polytechnic Institute"

Kyrpychova str., 2, Kharkiv, Ukraine, 61002

Copyright © 2020, O. Rezinin, A. Getman, S. Buryakovskiy, B. Kubrik

This is an open access article under the CC BY license

(<http://creativecommons.org/licenses/by/4.0>)

reciprocating inductor. In another case, windings move with a stationary inductor. Besides, a design option is possible with counter-moving windings and the inductor. Regardless of the electric generator purpose, modeling of the process of converting mechanical energy into electrical energy remains a difficult task even with a simplified form of impelling periodic mechanical motion [5]. This work is devoted to studying the magnetically active part of a linear electric generator in order to develop and experimentally verify an analytical model for the initial calculation of its main parameters.

## 2. Literature review and problem statement

A free-piston engine generator is an energy conversion device that combines an internal combustion engine and a linear electric machine. A chronological overview of its design options used is presented in [6]. Starting from the

middle of the last century, such energy sources were mainly used as air compressors and gas generators since, at that time, they provided advantages over conventional internal combustion engines and gas turbines. The efficiency of present-day free-piston engine generators is estimated up to 46 % at a power level of 23 kW [7]. Although prototypes show promising results in terms of engine performance and emissions, losses from friction and compression are still quite large. In recent years, a concept has been proposed for the use of a free-piston engine generator in the production of electric and hydraulic energy, mainly in hybrid electric vehicles [8]. However, most of the described prototypes based on such a concept have not been commercially successful.

As shown in [9], in the case of using one combustion chamber, to ensure the mechanical balancing of the system, it is necessary to use a shock absorber. This worsens the mass-dimensional indicators of the device. In addition, the generator itself must be used as a linear motor [10] which further complicates control of the engine-generator system. The design of the engine-generator based on two pistons is the most popular option for study [11]. This arrangement makes it possible to use a common moving part, namely, the magnet armature of the linear generator. In this case, the armature is mounted on a common rod with pistons at each end in two oppositely directed combustion chambers [12]. This arrangement eliminates the need for a rebound device since the combustion force in one drives the piston assembly to overcome compression pressure in the other cylinder. This makes it possible to obtain a compact device with a higher power to weight ratio. Total efficiency with this device design is about 50 % taking into consideration the thermal efficiency of the engine of 56 % and the efficiency of the generator of 96 % [13]. These studies are mainly focused on the optimization of engine parameters. However, no issues of the optimal operating mode and the corresponding design of the electric generator were examined.

A general requirement for various design options of a linear electric generator is the principle of creating maximum EMF (electric power) at a limited amplitude of reciprocal motion [14]. To increase the magnetic flux generated by the inductor and, accordingly, the EMF, permanent NdFeB magnets with a high value of residual induction are used in designing the generator armature. A complete calculation of parameters of such an electromechanical system is rather complicated [15] even after the introduction of additional simplifications for the expressions describing reciprocal motion and influence of the load current on it. Therefore, when modeling power plants with a linear electric generator, individual models for mechanical and electromagnetic subsystems are usually constructed.

As is known, analytical models have the widest possibilities in terms of analysis of the design and optimization of its parameters. The main difficulty in constructing analytical models of the electric generator is the search for an exact mathematical representation of the magnetic field of the magnetically active part of the generator. This is because of the fact that in the case of using a large number of simplifications in the description of the magnetic field and (or) the generator design, the issue of the model adequacy gets more acute [4]. Therefore, the representation of the magnetic field of the magnetically active part of the linear generator was chosen in the study as one of the possible ways of constructing its analytical model based on the cylindrical harmonic analysis.

---

### 3. The aim and objectives of the study

---

The study objective is to construct and experimentally verify the analytical model of a linear electric generator for the initial calculation of the main parameters of its magnetically active part. The model must provide a solution to the problem of optimizing the design of a linear electric generator by analytical calculation of geometric parameters of the permanent magnets and current windings.

To achieve this objective, the following tasks must be solved:

- to conduct a cylindrical harmonic analysis of the magnetic field of longitudinally moving permanent magnets of a cylindrical shape;
- to obtain direct expressions of magnetic flux generated by a set of coaxially arranged cylindrical magnets in a current winding of a simplified model of a linear electric generator;
- to verify the obtained expressions by comparing with the results of the analytical calculation of EMF induced in the current winding and oscillograms recorded applying the constructed physical model of a linear electric generator.

---

### 4. The materials and methods used in the study of a linear electric generator with permanent magnets

---

The study considered a linear electric generator in which armature is a moving part containing cylindrical permanent magnets of radius  $R$ . To carry out a cylindrical harmonic analysis of the magnetic field of the magnetically active part of the generator, the following simplifications and assumptions were made.

Assume that an armature with magnets moves along the axial axis  $z$  of the fixed winding according to a sinusoidal law:

$$z(t) = \ell \sin(\omega t), \quad (1)$$

where  $\ell$  is the amplitude of periodic translational motion (m);  $\omega$  is the cyclic frequency ( $s^{-1}$ );  $t$  is the time (s).

In this case, independence of the EMF induced in the stationary winding is assumed to depend on the current value in it. To simplify the model, the elements of the magnetic conductor that do not create magnetic flux but participate in its redistribution are not taken into consideration. Besides, contributions to the magnetic flux from non-magnetic structural elements and the motor remote from the windings are not taken into consideration.

---

### 5. The results obtained in the study of a magnetically active part of the linear electric generator

---

#### 5.1. Cylindrical harmonic analysis of the magnetic field of the permanent armature magnets

First, let us consider the magnetic flux  $\Phi(z)$  created by one cylindrical magnet in an axially positioned thin conducting circular circuit of radius  $r$  as a function of a coordinate  $z$  of the position of the magnet center relative to the circuit center. For a cylindrical magnet with height  $h$ , the range of movement of the end faces relative to the centrally located conducting circuit will be  $\pm(\ell+h/2)$  (Fig. 1). Use the following expressions for cylindrical harmonics of the scalar

potential of a cylindrical permanent magnet as a theoretical basis for the description of its magnetic field [16–20]:

– inside the cylinder ( $|z| \leq h/2, \rho \leq R$ ):

$$U_1 = J \left( z - \frac{2R}{\pi} \int_0^\infty \frac{1}{\lambda} K_1(\lambda R) I_0(\lambda \rho) \sin \lambda \frac{h}{2} \sin \lambda z d\lambda \right); \quad (2)$$

– outside the cylinder ( $|z| \geq h/2, \rho \leq R$ ):

$$U_1 = -\frac{2JR}{\pi} \int_0^\infty \frac{1}{\lambda} K_1(\lambda R) I_0(\lambda \rho) \sin \lambda \frac{h}{2} \sin \lambda z d\lambda; \quad (3)$$

– at  $\rho > R$ :

$$U_2 = \frac{2JR}{\pi} \int_0^\infty \frac{1}{\lambda} I_1(\lambda R) K_0(\lambda \rho) \sin \lambda \frac{h}{2} \sin \lambda z d\lambda, \quad (4)$$

where  $J$  is the residual magnetization (A/m);  $I_n, K_n$  are the modified Bessel functions;  $\rho, z$  are the cylindrical coordinates of the magnetic field observation point.

The following formula for functional dependence of the magnetic flux on time can be obtained by calculating magnetic induction [17] using (2) to (4) and performing integration over the circuit area:

$$\Phi(t) = 4\mu_0 r J R \times \int_0^\infty \frac{1}{\lambda} K_1(\lambda r) I_1(\lambda R) \times \sin \left( \lambda \frac{h}{2} \right) \cos(\lambda z(t)) d\lambda. \quad (5)$$

An example of such a dependence (5) on time taken as a half-period (phase span from  $-\pi/2$  to  $+\pi/2$ ) is shown in Fig. 1 by a dashed line. For this example, the following values were used as the initial calculation data:  $J=1.09 \cdot 10^6$  A/m,  $\ell=0.02$  m,  $h=0.02$  m,  $\omega=2\pi \cdot 16$  s<sup>-1</sup>,  $r=0.026$  m. In order to use the common scale of the abscissa axis for movement and time, a linear coefficient of time recalculation ( $4/\pi$ ) was introduced in Fig. 1. Comparing the dashed graph and the dot graph for the dependence of  $\Phi$  on the  $z$  coordinate, it can be pointed out that nonlinearity of the armature movement in time does not change the maximum value of magnetic flux in the circuit. Besides, it follows from the form of dependence of  $\Phi$  on the coordinate that the greatest steepness of the magnetic flux function corresponds to positions of the end faces inside the circuit plane (corresponding points on the graphs  $z=\pm 0.01$  m and  $4t/\pi \approx \pm 0.0066$  s).

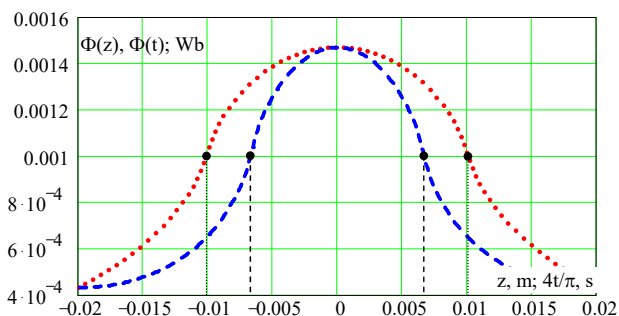


Fig. 1. The behavior of magnetic flux in a circular circuit when a permanent cylindrical magnet is moving through it

A graph constructed for the time dependence of the EMF  $E$  induced in a circular circuit based on the following formula is shown in Fig. 2.

$$E(t) = 4\mu_0 \omega \ell r J R \cos(\omega t) \times \int_0^\infty K_1(\lambda r) I_1(\lambda R) \sin \left( \lambda \frac{h}{2} \right) \sin(\lambda \ell \sin(\omega t)) d\lambda. \quad (6)$$

The functional dependence of EMF on time (6) has two peaks of the same amplitude but opposite in sign corresponding to the moments when the end faces of the magnet cross the circuit plane. In other magnet positions, the amplitude of the induced EMF is 3 to 5 times smaller. It is zero when centers of the circuit and the cylindrical magnet coincide.

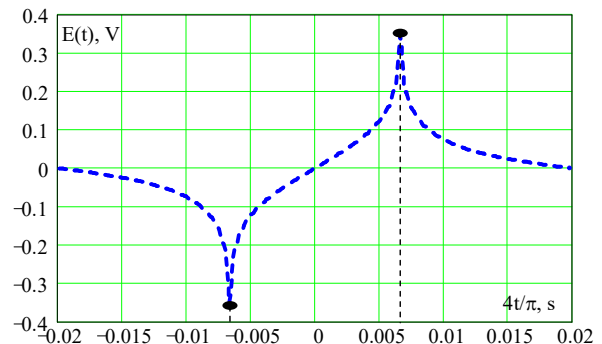


Fig. 2. EMF induced in a circular circuit during periodic translational movement of a permanent magnet

Thus, to generate more energy (to create more EMF peaks) during the linear movement of the armature, it seems rational to use several short magnets instead of one long magnet. In this case, poles of the magnets should be oriented pairwise opposite to provide an increase in the number of EMF peaks with the same movement of the armature. According to dependence (6), this change in geometric parameters (length reduction) should change the amplitude magnitude of the EMF peak. However, the number of short magnets can be chosen so that the change in amplitude of the EMF peak is insignificant, for example, less than 10 % as for the case with three magnets (solid line in Fig. 3).

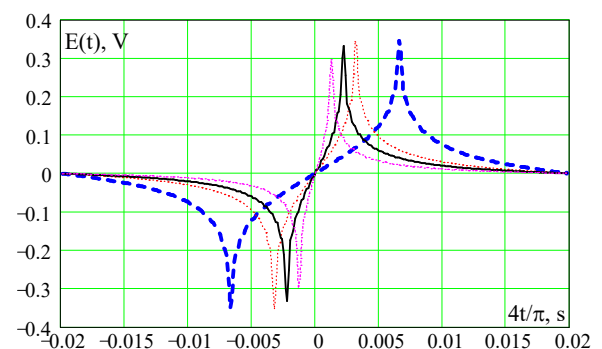


Fig. 3. The behavior of the EMF in a circular circuit at various values of height of the moving cylindrical magnet

In addition, a decrease in the magnitude of the EMF amplitude can be compensated by a small increase in the diameter of cylindrical magnets. According to the graph shown in Fig. 4, the dependence of the magnitude of the EMF peak  $E(t)$  on radius  $R$  of cylindrical magnets is almost linear (as before, consider it equal to  $r$ , the radius of the conducting circular circuit). A more important factor that

significantly reduces the amplitude of the peaks when using an armature with several magnets is constituted by their mutual negative effect on the induced magnetic flux since the pole orientation of the magnets and the corresponding contributions to the magnetic flux of two adjacent magnets are opposite.

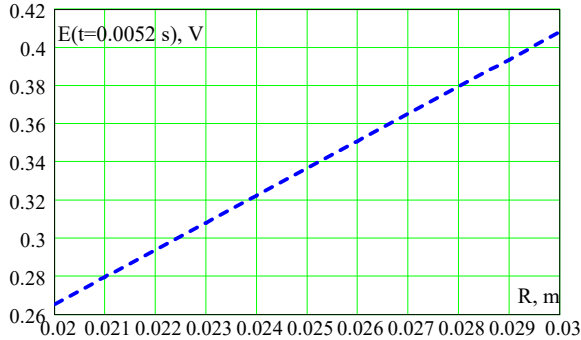


Fig. 4. Dependence of the maximum EMF value on radius of the moving cylindrical magnet

An example of such a decrease in amplitude of the magnetic flux induced in a circular circuit by four axially arranged cylindrical magnets is shown in Fig. 5. The formula for calculating the total magnetic flux  $\Phi_{\Sigma}$  can be obtained on the basis of (5) in a form of a sum of magnetic fluxes induced by four oppositely oriented magnets moved along the axis:

$$\Phi_{\Sigma}(t) = \Phi(s_1 + z(t)) - \Phi(s_2 + z(t)) + \Phi(s_3 + z(t)) - \Phi(s_4 + z(t)), \quad (7)$$

where  $s_1, s_2, s_3, s_4$  are displacements of initial positions of the corresponding magnet center relative to the circular circuit center. For Fig. 5, the displacement values are equal to 0 m, 0.02 m, 0.04 m, 0.06 m.

The following conclusion can be drawn from a comparison of the magnetic flux maxima in Fig. 1 (one magnet) and in Fig. 5 (total  $\Phi_{\Sigma}$  of the four magnets). The smallest amplitude of the magnetic flux peaks is characteristic of the position of two middle magnets in the circular circuit center since two adjacent magnets have opposite poles for each of them. On the other hand, the magnetic flux generated by the outermost magnets actually reduces that of only one adjacent magnet, so when their center coincides with the circular circuit center, the flux amplitude turns out to be larger. By taking the time derivative of the dependence of the total magnetic flux in (7), a typical dependence of EMF  $E(t)$  can be obtained. For the case of the initial position of the first magnet in the plane of the circular circuit, a graph of the EMF induced by movement of the four magnets is shown in Fig. 6, 7.

The time interval from 0 s to 0.015 s in the graph of Fig. 6 corresponds to movement from the first magnet center to the second magnet center. The subsequent time interval from 0.015 s to 0.03 s corresponds to movement from the second magnet center to the first magnet center. The final time interval from 0.03 s to 0.06 s corresponds to moving away (up to 0.045 s) and the subsequent approach of the four magnets to the circular circuit plane.

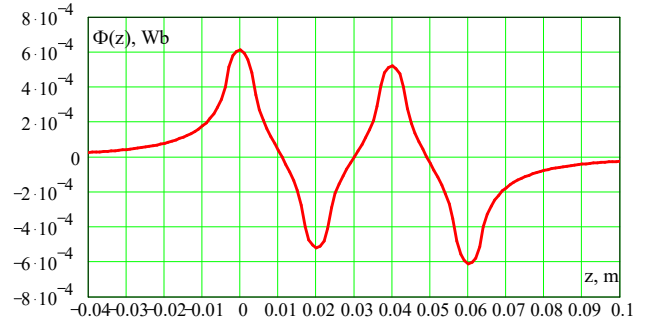


Fig. 5. The behavior of magnetic flux in a circular circuit during periodic movement of an armature of four magnets

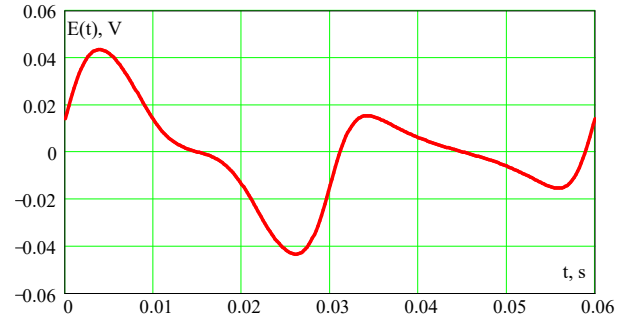


Fig. 6. Calculated EMF in a circular circuit during periodic movement of the armature composed of four magnets

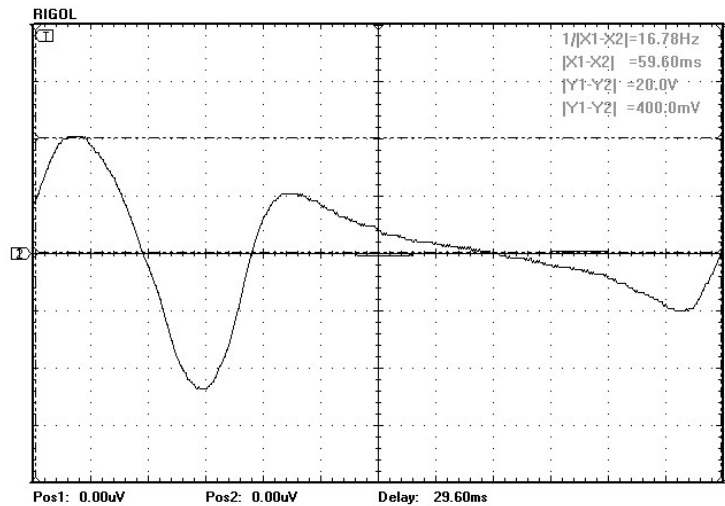


Fig. 7. Photograph of the EMF oscillogram in a circular winding of one hundred turns during periodic movement of the armature composed of four magnets and a voltage divider 1 to 10 turned on

In practice, the use of continuous cylindrical magnets is limited by properties of mechanical strength of the magnetic materials used which provide a large value of residual magnetization. To increase strength, cylindrical annular permanent magnets are used in the armature design. They are mounted on a transporting steel rod having a small value of magnetic susceptibility. Therefore, in a first approximation, to simulate magnetic flux  $\Phi_c$  of the annular cylindrical magnets with internal radius  $R_m$ , the difference of magnetic fluxes obtained from (5) can be used:

$$\Phi_c(t) = 4\mu_0 t f \int_0^{\infty} \lambda K_1(\lambda r) [R I_1(\lambda R) - R_m I_1(\lambda R_m)] \times \sin\left(\lambda \frac{h}{2}\right) \cos(\lambda z(t)) d\lambda. \quad (8)$$

The presence of a cylindrical cavity inside the magnet decreases the magnetic flux created by it and, accordingly, EMF in a circular conducting circuit. The relative decrease in the maximum magnetic flux of an annular magnet in comparison with a continuous cylindrical magnet of the same external diameter and height is shown in Fig. 8 for various diameter to height ratios.

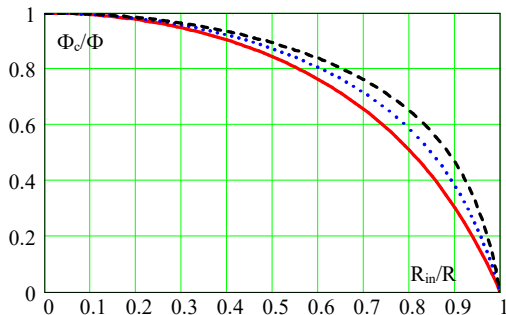


Fig. 8. Dependence of magnetic flux in a circular circuit on an increase in the internal radius of the annular cylindrical magnet

In Fig. 8, ratios of the cylindrical magnet height to its outside diameter are as follows: 1 to 20 for the dashed line; 1 to 10 for the dotted line; 1 to 5 for the solid line. It follows from an analysis of the three graphs in Fig. 8 that when inside radius  $R_{in}=0.4 R$ , the difference between the magnetic flux generated by the annular magnet and that of the continuous cylindrical magnet of the same diameter does not exceed 10 %.

**5. 2. Analysis of magnetic flux coupled to the current winding**

The fundamental difference between geometrical parameters of an actual circular current winding of a linear electric generator and that of the considered circular circuit consists in presence of a gap between the permanent magnets and the winding. Presence of the gap technologically necessary to ensure movement of the armature and laying the winding turns (a larger radius of the winding turns compared to the magnet radius) results in a partial flux closure inside the winding. This leads to a decrease in the total magnetic flux linkage created by the magnets with windings. In particular, based on (5), graphs of the dependence of relative decrease in the magnetic flux generated by one centrally positioned magnet on the relative increase in the radius of the circular circuit can be constructed for one turn of radius  $r$  (Fig. 9).

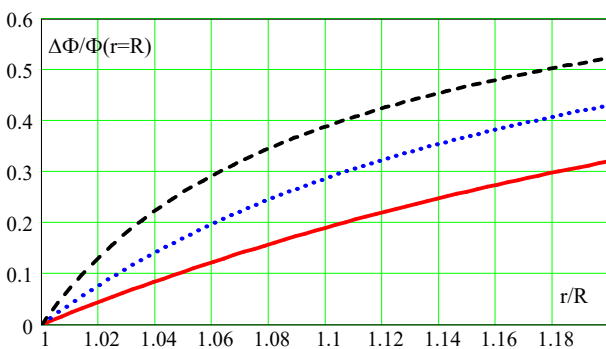


Fig. 9. Dependence of the relative loss of magnetic flux on an increase in the radius of a circular circuit

As follows from the graph shown in Fig. 9 by a dashed line, when the ratio of the magnet diameter to its height is 20 to 1 and the gap is 3 % of the magnet radius, the magnitude of the magnetic flux coupled to the circular circuit will decrease by 20 % relative to its maximum possible value. The same decrease in magnetic flux when the ratio of the magnet diameter to its height is 10 to 1 (a dotted line) was observed with a gap of 6 % of the magnet radius. Analysis of the graph shown in Fig. 9 by the solid line constructed for the 5 to 1 ratio of the magnet diameter to its height shows a 20 % relative decrease in magnetic flux at a gap of 11 % of the magnet radius.

Similar to the case with a circular circuit, the presence of a gap between the actual winding and the magnets will lead to a significant decrease in the magnetic flux coupled to a multi-turn winding. In addition, it is obvious that with an increase in the outside diameter of the winding, the average value of magnetic flux in its turns will decrease as well. Therefore, the radial size of the winding ( $\Delta r=r_{out}-r_{in}$  is the difference between its external and internal radii) should be limited proceeding from an analysis of the increase in relative losses of the magnetic flux with an increase in the winding radius. In a complete analogy with Fig. 9, Fig. 10 shows a reduction of the average value of the magnetic flux coupled to a flat disk-shaped winding. The decrease in magnetic flux is shown as a function of the relative outside radius of the winding at an inside radius  $r_{in}$  of 107 % relative to the permanent magnet radius  $R$ .

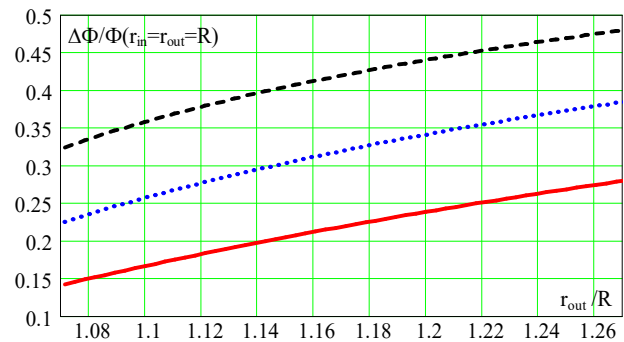


Fig. 10. Dependence of the relative decrease in magnetic flux with an increase in the relative outside radius of the winding

It follows from an analysis of the three dependences of the magnetic flux losses shown in Fig. 10 that a decrease in relative thickness of the magnet by half leads to a 10 % increase in flux linkage losses. A further four-fold decrease in thickness leads to a 20 % increase in losses. Moreover, the increase in the flux linkage loss with growth of outside winding radius is almost independent of the relative thickness of the permanent magnet. The graphs in Fig. 10 substantiate the need for a magnetic conductor enveloping the winding to reduce the level of flux linkage losses. This is especially true for thin cylindrical magnets with a diameter to height ratio of 10 to 1 or more.

Another limitation imposed on the geometry of the cylindrical winding is associated with a change in the initial EMF phase in the coil turns with different longitudinal coordinates. The difference in initial phases of the EMF induced in longitudinally laid turns is determined by the difference in distance between the turns and the magnets with a translational nature of the armature movement according to (1) and (6). The difference in the geometric position of turns leads to a difference in instantaneous values of the magnetic flux and initial phases of the EMF in them, and,

as a result, to a decrease in the total EMF of the winding. Therefore, it is advisable to limit the longitudinal size of the winding in such a way as to minimize the spread of initial phases of its outermost turns. For example, the longitudinal size of the winding can be limited to a value equal to the height of cylindrical magnets. Then the typical spread of initial phases of the EMF induced in opposite outermost turns of the winding will lead to a 20 % decrease in the total EMF amplitude compared to the doubled amplitude of the EMF in a turn (Fig. 11). Fig. 11, 12 show calculated and experimental time dependences of the instantaneous EMF value. Also, the dashed and dotted lines in Fig. 11 show the EMF induced in each of two identical circular turns positioned axially at a distance equal to the height of the cylindrical armature magnets. The total EMF of two turns spaced by 5 mm is shown by the solid line in Fig. 11.

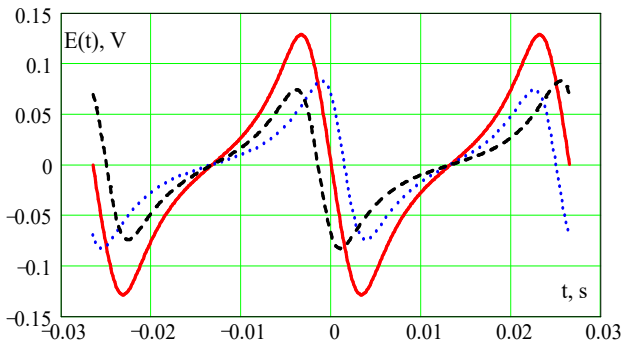


Fig. 11. Time dependence of the EMF at various initial positions of the circular circuit

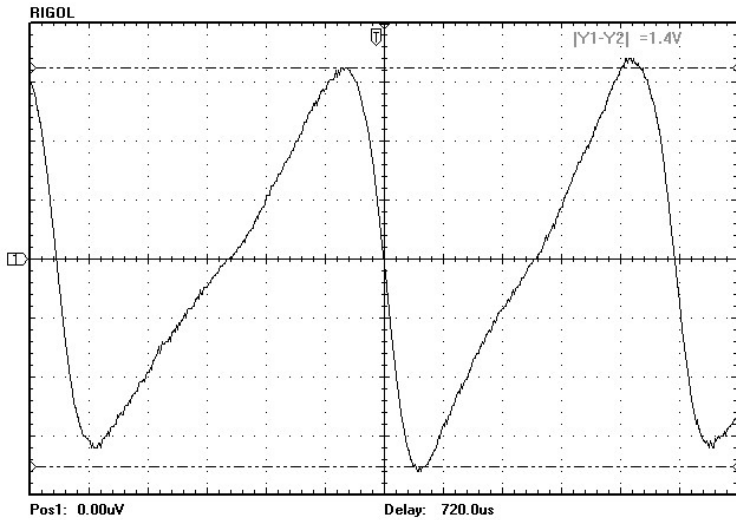


Fig. 12. Photograph of the EMF oscillogram obtained when the voltage divider 1 to 10 is turned on in a circuit of a winding of one hundred turns; the longitudinal coordinate of the winding corresponds to initial position of the second magnet

When observing the total EMF induced in the cylindrical winding and that shown in Fig. 11, 12, closeness of its shape to a sinusoidal dependence can be seen. To increase the generated power, such windings (sections) should be located above each cylindrical armature magnet and in its middle position and switched in series opposing to each other. Then the problem of calculating the total EMF of the generator will be reduced to multiplying the number of such winding sections by the calculated value of the EMF induced by one section.

### 5.3. Verification of the obtained expressions using the constructed physical model of a linear electric generator

To verify the adequacy of the proposed analytical model of the magnetically active part of a linear electric generator, a physical model was constructed and studied. Its appearance is shown in Fig. 13. To ensure periodic translational movement of armature 1 relative to winding 2 on stationary cylinder 3, electric motor 4 was used with flywheel 5 to which connecting rod 6 was eccentrically attached. During rotation of the flywheel, a periodic translational movement with an amplitude of 0.02 m and a frequency of 16 Hz was transmitted to shaft 7. Thus, the law of periodic movement of the armature was ensured according to (1).

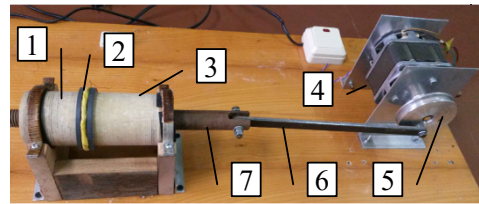


Fig. 13. General view of the physical model: 1 - magnets; 2 - winding; 3 - bearing cylinder; 4 - electric motor; 5 - flywheel; 6 - connecting rod; 7 - shaft

Four permanent annular cylindrical magnets with a height  $h=0.007$  m, outside and inside radii  $R=0.026$  m and  $R_{in}=0.01$  m, respectively, were used in the constructed physical model. According to Fig. 14, the distance between centers of the axially arranged magnets was equal to the amplitude of periodic motion of 0.02 m. A 0.005 m dia. winding containing 100 turns was mounted on a 0.06 m dia. bearing cylinder so that its center coincided with the center of one of the permanent armature magnets. To record instantaneous values of the EMF generated in the winding, a RIGOL DS1000B digital oscilloscope was used.

Typical screenshots of oscillograms obtained in experiments with a physical model are shown in Fig. 7, 12. For direct quantitative comparison of the oscillograms with the calculated dependences, it should be taken into consideration that the experimental data were obtained for a winding of one hundred turns with the voltage divider 1 to 10 turned on. Therefore, to obtain the EMF induced in one averaged winding turn, the measured voltage should be divided by 10. Whence it follows that magnitude of the peak EMF induced in one averaged winding turn is  $(4.3/2) \times (400/2) = 430$  mV (Fig. 7) and  $1.4/2 = 0.7$  V for the oscillation amplitude (Fig. 12).

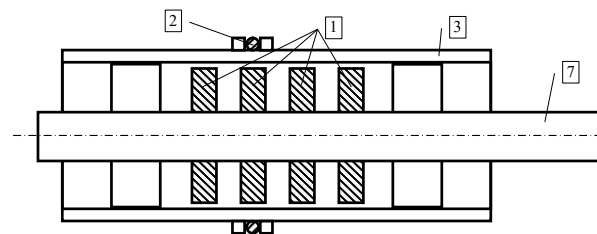


Fig. 14. Arrangement of permanent magnets 1 of the armature relative to winding 2

## 6. Discussion of the results obtained from constructing an analytical model of a linear electric generator

Thus, based on the proposed analytical model, initial values of geometric parameters of the current winding can be calculated, and then the number of the winding turns is calculated based on its specified impedance. Next, based on (6), one can obtain the value of the EMF induced in each section of a cylindrical winding of a linear electric generator and calculate the generated electric power which is proportional to the square of the frequency of periodic translational movement of the armature. At a periodic law of motion of the armature (1), the generated electric power quadratically increases with increasing amplitude of displacement  $\ell$ . In other words, with an increase in the armature stroke length by a factor of two, power will increase by a factor of four. A similar increase in power will be with an increase in the number of cylindrical magnets (while maintaining the longitudinal size of the armature).

To plot graphs and calculate values of the integrals in expressions containing modified Bessel functions, specialized mathematical software package MathCAD16 was used. In this case, the property of fast decay of the Bessel functions was used to calculate the integrals from (5) to (7) in which the infinite upper limit was replaced by a finite number of the order of  $10^3$ .

A comparison of the experimentally obtained oscillograms with those calculated on the basis of the analytical model has shown their insignificant discrepancy. The discrepancy in calculations is caused by the use of averaged coordinates of a single turn under an assumption of using a sufficiently thin winding and a scatter of residual magnetization of permanent magnets.

The model features a field character as it is based on direct analytical expressions for the EMF in the current winding, which allows one to find rational values of design parameters of the magnetically active part of the electric generator. The use of cylindrical harmonic analysis of the magnetic field has made it possible to examine in detail the scatter fields which are usually neglected in other models. In particular, the model makes it possible to consider the relative loss of magnetic flux in the current winding as a quantitative criterion of effectiveness of the generator design option. In addition, based on the periodic law of armature movement, the model makes it possible to calculate time dependence of the EMF induced in the current winding. This is important from the point of view of optimizing the use of generated electricity.

The model can be further refined by introducing in (6) to (8) integration (or summation) in terms of coordinates of all winding turns. It is also obvious that the model can be adapted for the case of a more complex law of periodic mechanical movement of the armature characteristic of a free-piston generator.

However, the preliminary nature of the analysis based on the presented simplified model of an electric generator without a magnetic conductor should be taken into consideration. The complexity of the spatial distribution of the magnetic field of the magnetic conductor does not allow an analytical description without additional simplifications. Their introduction negatively affects the model accuracy. Therefore, it seems rational to use numerical models for the exact calculation of power produced by the generator with its structural parameter values obtained using an analytical model.

## 7. Conclusions

1. As a result of a cylindrical harmonic analysis of the magnetic field created by permanent armature magnets, an analytical model of the magnetically active part of a linear electric generator was developed. It features the inclusion of losses in a form of scatter fields in the analysis of magnetic flux in the current winding as well as the possibility of representing instantaneous EMF values in accordance with the law of mechanical movement of the armature.

2. Based on the mathematical apparatus of cylindrical harmonics of the scalar potential of the magnetic field, relations were obtained for initial calculation and analysis of parameters of the armature and current winding of the electric generator. The relationships make it possible to search for the optimal design of the generator by the criterion of maximum efficiency of conversion of mechanical energy into an electrical one.

3. Using the constructed physical model of a linear electric generator, experimental studies were conducted. They have confirmed the adequacy of the proposed analytical model. Within the framework of the stipulated assumptions, the accuracy of the analytical model is limited by the scattering of values of residual induction of the permanent magnets. For permanent magnets from one batch, the relative difference in residual induction is within 5%. Parameters of the magnetically active part of the armature calculated using the model are basic for subsequent analysis and calculation of a magnetic conductor design for a linear electric generator.

## References

- Kondratenko, I. P., Rashchepkin, A. P., Vashchishyn, D. D. (2010). Rozrakhunok elektrorushyynoi syly liniynoho heneratora dlia peretvorennia enerhiyi khvyl. *Visnyk Kremenchutskoho derzhavnogo universytetu im. M. Ostrohradskoho*, 4 (1), 72–75.
- Slychenko, A. A., Klyuev, K. M. (2005). Sudovoy lineyniy dizel'-generator dlya propul'sivnyh kompleksov. *Sudovye energeticheskie ustanovki*, 12, 145–151.
- Miao, Y., Zuo, Z., Feng, H., Guo, C., Song, Y., Jia, B., Guo, Y. (2016). Research on the Combustion Characteristics of a Free-Piston Gasoline Engine Linear Generator during the Stable Generating Process. *Energies*, 9 (8), 655. doi: <https://doi.org/10.3390/en9080655>
- Menzhinski, A. B., Malashin, A. N., Sukhodolov, Y. V. (2019). Experimental Verification of the Adequacy of Mathematical Model of the Reciprocating Electric Electromagnetically Excited Generator. *ENERGETIKA. Proceedings of CIS Higher Education Institutions and Power Engineering Associations*, 62 (2), 168–176. doi: <https://doi.org/10.21122/1029-7448-2019-62-2-168-176>
- Kondratenko, I. P., Rashchepkin, A. P., Vashchishin, D. D. (2012). A dynamic model of a linear permanent magnet generator for converting wave energy. *Tekhnichna elektrodynamika*, 2, 113–114. Available at: [http://techned.org.ua/2012\\_2/st54.pdf](http://techned.org.ua/2012_2/st54.pdf)

6. Mikalsen, R., Roskilly, A. P. (2007). A review of free-piston engine history and applications. *Applied Thermal Engineering*, 27 (14-15), 2339–2352. doi: <https://doi.org/10.1016/j.applthermaleng.2007.03.015>
7. Jia, B., Smallbone, A., Mikalsen, R., Shivaprasad, K. V., Roy, S., Roskilly, A. P. (2019). Performance Analysis of a Flexi-Fuel Turbine-Combined Free-Piston Engine Generator. *Energies*, 12 (14), 2657. doi: <https://doi.org/10.3390/en12142657>
8. Jia, B., Zuo, Z., Tian, G., Feng, H., Roskilly, A. P. (2015). Development and validation of a free-piston engine generator numerical model. *Energy Conversion and Management*, 91, 333–341. doi: <https://doi.org/10.1016/j.enconman.2014.11.054>
9. Kosaka, H., Akita, T., Moriya, K., Goto, S., Hotta, Y., Umeno, T., Nakakita, K. (2014). Development of Free Piston Engine Linear Generator System Part 1 - Investigation of Fundamental Characteristics. SAE Technical Paper Series. doi: <https://doi.org/10.4271/2014-01-1203>
10. Goto, S., Moriya, K., Kosaka, H., Akita, T., Hotta, Y., Umeno, T., Nakakita, K. (2014). Development of Free Piston Engine Linear Generator System Part 2 - Investigation of Control System for Generator. SAE Technical Paper Series. doi: <https://doi.org/10.4271/2014-01-1193>
11. Feng, H., Guo, C., Yuan, C., Guo, Y., Zuo, Z., Roskilly, A. P., Jia, B. (2016). Research on combustion process of a free piston diesel linear generator. *Applied Energy*, 161, 395–403. doi: <https://doi.org/10.1016/j.apenergy.2015.10.069>
12. Jia, B., Smallbone, A., Zuo, Z., Feng, H., Roskilly, A. P. (2016). Design and simulation of a two- or four-stroke free-piston engine generator for range extender applications. *Energy Conversion and Management*, 111, 289–298. doi: <https://doi.org/10.1016/j.enconman.2015.12.063>
13. Mikalsen, R., Roskilly, A. P. (2008). The design and simulation of a two-stroke free-piston compression ignition engine for electrical power generation. *Applied Thermal Engineering*, 28 (5-6), 589–600. doi: <https://doi.org/10.1016/j.applthermaleng.2007.04.009>
14. Jia, B., Tian, G., Feng, H., Zuo, Z., Roskilly, A. P. (2015). An experimental investigation into the starting process of free-piston engine generator. *Applied Energy*, 157, 798–804. doi: <https://doi.org/10.1016/j.apenergy.2015.02.065>
15. Jia, B., Smallbone, A., Feng, H., Tian, G., Zuo, Z., Roskilly, A. P. (2016). A fast response free-piston engine generator numerical model for control applications. *Applied Energy*, 162, 321–329. doi: <https://doi.org/10.1016/j.apenergy.2015.10.108>
16. Watson, G. N. (1922). *A treatise on the theory of Bessel functions*. Cambridge: Cambridge Univ. Press, 804. Available at: [https://www.forgottenbooks.com/de/download/ATreatiseontheTheoryofBesselFunctions\\_10019747.pdf](https://www.forgottenbooks.com/de/download/ATreatiseontheTheoryofBesselFunctions_10019747.pdf)
17. Smythe, W. (1950). *Static and Dynamic Electricity*. McGraw-Hill, 623. Available at: <https://archive.org/details/StaticAndDynamicElectricity/page/n95/mode/2up>
18. Gray, A., Mathews, G. B. (1895). *A treatise on Bessel functions and their applications to physics*. Macmillan and Co., 316. Available at: <https://archive.org/details/treatiseonbessel00grayuoft/page/n10/mode/2up>
19. Getman, A. V., Konstantinov, A. V. (2013). Cylindrical harmonics of magnetic field of linear magnetized cylinder. *Tekhnichna elektrodynamika*, 1, 3–8. Available at: [http://techned.org.ua/2013\\_1/st1.pdf](http://techned.org.ua/2013_1/st1.pdf)
20. Getman, A. V., Konstantinov, A. V. (2011). Cylindrical harmonics of magnetic field of a uniformly magnetized cylinder. *Elektrotehnika i Elektromekhanika*, 5, 51–53. Available at: [http://repository.kpi.kharkov.ua/bitstream/KhPI-Press/13573/1/EE\\_2011\\_5\\_Get%27man\\_Tsilindricheskiye.pdf](http://repository.kpi.kharkov.ua/bitstream/KhPI-Press/13573/1/EE_2011_5_Get%27man_Tsilindricheskiye.pdf)